

Received 5 October 2023, accepted 2 November 2023, date of publication 14 November 2023,  
date of current version 22 November 2023.

Digital Object Identifier 10.1109/ACCESS.2023.3333046

## RESEARCH ARTICLE

# Performance Analysis of Bidirectional Multi-Hop Vehicle-to-Vehicle Visible Light Communication

SOUAD REFAS<sup>1</sup>, DALILA ACHELI<sup>2</sup>, SELMA YAHIA<sup>1</sup>, (Member, IEEE), YASSINE MERAIHI<sup>1</sup>,  
AMAR RAMDANE-CHERIF<sup>3</sup>, VAN NHAN VO<sup>4,5</sup>, AND TU DAC HO<sup>6,7</sup>, (Senior Member, IEEE)

<sup>1</sup>LIST Laboratory, University of M'Hamed Bougara Boumerdes, Boumerdes 35000, Algeria

<sup>2</sup>LAA Laboratory, University of M'Hamed Bougara Boumerdes, Boumerdes 35000, Algeria

<sup>3</sup>LISV Laboratory, University of Versailles Saint-Quentin-en-Yvelines, 78140 Vélizy-Villacoublay, France

<sup>4</sup>Faculty of Information Technology, Duy Tan University, Da Nang 550000, Vietnam

<sup>5</sup>Institute of Research and Development, Duy Tan University, Da Nang 550000, Vietnam

<sup>6</sup>Faculty of Engineering Science and Technology, UiT The Arctic University of Norway, 9019 Narvik, Norway

<sup>7</sup>Faculty of Information Technology and Electrical Engineering, Norwegian University of Science and Technology (NTNU), 7010 Trondheim, Norway

Corresponding authors: Tu Dac Ho (tu.d.ho@uit.no) and Souad Refas (s.refas@univ-boumerdes.dz)

This work was supported by the UiT-The Arctic University of Norway.

**ABSTRACT** Vehicular visible light communication (VVLC) has emerged as a promising field of research, garnering considerable attention from scientists and researchers. VVLC offers a potential solution to enable connectivity and communication between travelling vehicles along the road by using their existing headlights (HLs) and taillights (TLs) as wireless transmitters and integrating photodetectors (PDs) within the car front or car-back as wireless receivers. However, VVLC encounters more challenges than indoor VLC, particularly in vehicle-to-vehicle (V2V) communication, where vehicle mobility disrupts the establishment of direct communication links. To address this, we propose a multi-hop relay system wherein intermediate vehicles act as wireless relays to maintain a line-of-sight (LoS) link. In this paper, we investigate the performance of a bidirectional multi-hop relay V2V-VLC system that operates in both the forward and backward directions. Based on realistic ray tracing channel models, we derive a closed-form expression for the full bidirectional communication range. We also analyze how the transceiver's parameters and the number of relays affect the system performance. Our results show that the proposed bidirectional multi-hop relay system can extend the direct transmission range by more than 19 m with only a hop relay.

**INDEX TERMS** Vehicular visible light communication, unidirectional and bidirectional multi-hop vehicle-to-vehicle communications, full bidirectional connectivity range, transceiver parameters.

## I. INTRODUCTION

Vehicular communication has recently attracted much interest from scientists as one of the key enabling technologies for Intelligent Transportation Systems (ITSs) [1], [2]. Vehicular communication encompasses various wireless communication technologies and services with various connectivity links. These include vehicle-to-infrastructure (V2I), vehicle-to-vehicle (V2V), infrastructure-to-vehicle (I2V), and vehicle-to-pedestrian (V2P) communication, collectively known as vehicle-to-everything (V2X) [3].

The current deployment of V2X applications mainly relies on the use of radio frequency (RF)-based solutions

The associate editor coordinating the review of this manuscript and approving it for publication was Jiankang Zhang.

such as Dedicated Short-Range Communications (DSRC) [4], [5], Cellular Vehicle-to-Everything communication (C-V2X) [6], [7], Advanced Driver Assistance Systems (ADAS) [8], [9], and Long-Term Evolution-Vehicle (LTE-V) technologies [10]. However, a wide prevalence of ITSs is highly expected, making the corresponding limited radio-frequency bands rapidly suffer from high interference and congestion levels, especially in medium and high node density situations [11]. Therefore, alternative or complementary solutions to RF-based technology have become indispensable [12], [13].

One of the most promising solutions is the deployment of visible light communication (VLC) technology [14], [15]. Such technology is based on the simultaneous use of light-emitting diodes (LEDs) as illumination devices and

wireless data transmitters. Moreover, the rapid use of LEDs in automotive headlights (HLs), taillights (TLs), road traffic, and street lights make VLC a natural vehicular connectivity solution [16]. Vehicular VLC (VVLC) technology has received increasing interest in recent years. As a result, several research directions such as but not limited to channel modelling [17], [18], [19], [20], [21], physical layer design [22], [23], [24], medium access control (MAC) protocols [25], [26], [27], and hybrid RF-VLC systems [28], [29], have been investigated.

Because adopting VLC technology in vehicular applications is still relatively new, it is essential to explore its capabilities and limitations [30]. This is particularly important for V2V VLC applications, which is the focus of this paper. In this regard, several critical questions remain open, including: *i*) What is the reliable communication range that V2V VLC technology can support? *ii*) How can this range be extended? *iii*) What is the budget required to achieve this reliable communication range? *iv*) How does the communication speed affect this range? In addition, to answer these questions accurately, it is essential to use realistic channel models for V2V VLC systems, as this is the primary stage of the communication system design.

It is worth noting that both forward and backward V2V communications are vital in future ITSs to enhance road safety, traffic efficiency, and overall driving experience by enabling vehicles to share critical information and cooperate in real-time. For instance, backward V2V communication is used in Rear-End Collision Warning to warn each other about potential rear-end collision risks, enhancing safety. In contrast, forward V2V communication is used in Cooperative Collision Avoidance to share warnings and alerts about potential hazards, reducing the risk of accidents. Also, in platoon V2V coordination, backward V2V communication is required in forming and managing platoons of vehicles, allowing the platoon leader to communicate with platoon members (utilizing multi-hop relaying techniques). At the same time, a forward link is essential to allow platoon members to exchange emergency and safety information with the platoon leader. Forward and backward V2V communications can then enable precise coordination of speed, acceleration, and braking among vehicles in the platoon, improving traffic flow and fuel efficiency.

While there have been many efforts in the literature to develop V2V VLC channel models, earlier works [31], [32] relied on the ideal Lambertian channel model with a line-of-sight (LoS). However, this model cannot represent the light pattern of actual cars with asymmetrical distribution patterns, as stipulated by Federal Motor USA Vehicle Safety Standards [33]. Therefore, the piece-wise Lambertian model was introduced to represent the asymmetrical distribution of the scooter's light [34], and similar models were developed for the asymmetrical distribution of HLs and TLs based on the measured intensity distribution [35], [36]. Furthermore, the non-sequential ray-tracing technique is also used as

an alternative channel modelling approach. This approach allows the propagation of light rays in complex geometries with a high order of reflections and facilitates practical optics design [37]. Based on this approach, the channel path loss of V2V VLC systems can be derived and used to obtain the total communication distance. However, most existing studies consider the availability of the direct LoS link [38], which cannot be maintained in all practical V2V scenarios [39]. This limitation has prompted deploying multi-hop relay systems as alternative solutions, which can relax the LoS constraint and significantly extend the communication range.

## II. RELATED WORK

Multi-hop communication was initially proposed for RF-based V2V communications as [40] and [41], where the intermediate cars serve as relay nodes, receive the signal from the source vehicle, decode it, and relay it to reach the destination vehicle. This relaying process can significantly increase the communication range and enable connectivity even when the unavailable LoS links between the source and destination. Vehicular VLC with multi-hop schemes has received little attention in the past [49]. However, there have been recent proposals for integrating multi-hop schemes into various vehicular VLC systems [26], [42], [43], [44], [45], [46], [50]. For example, in [42] and [43], the authors investigated a forward link in a multi-hop V2V system, considering that the HLs have a Lambertian pattern, which differs from the asymmetric profiles of real HLs. To consider such an asymmetrical pattern and calculate the attainable distance for the V2V link, the authors in [44] used a ray-tracing approach to obtain a linear path loss model and then applied it to investigate the forward link performance. Moreover, the authors in [45] investigated hybrid I2V-V2V systems, in which the vehicle receives the signal, transmitted by the traffic light, and then re-transmitted by its rear lights to the car following it. Another effort in [26], based on the exponential path loss channel model in [46], investigated a multi-hop V2V VLC system considering only the forward link. Also, this work focuses only on the medium access control (MAC) layer and does not discuss or provide analytical expressions for the maximum feasible communication range. In addition to simulation studies, some experimental attempts on multi-hop V2V-VLC systems have been presented in [47] and [48]. Nevertheless, these studies have yet to derive the maximum achievable distance.

It can be further noticed that the works above as in [26], [42], [43], [44], [45], [46], [47], and [48] have built multi-hop V2V with VLC based on the assumption that only a unidirectional link is considered (either forward or backwards). To provide a precise characterization of the multi-hop V2V-VLC system, it is necessary to consider the bidirectional connectivity where the vehicle uses its HLs for the forward connection and its TLs for the backward connection.

TABLE 1. The list of most relevant literature.

| Reference  | scenario | Contribution  |
|------------|----------|---|
| [40], [41] | V2V-RF   | Multi-hop communication initially proposed for RF-based V2V communications, where the intermediate cars serve as relay nodes  |
| [42], [43] | V2V-VLC  | The authors investigated only a forward link in a multi-hop V2V system, and considering that the HLs have a Lambertian pattern, which differs from the asymmetric profiles of real HLs or TLs |
| [44]       | V2V-VLC  | The authors considered a channel path loss model works only for shorter distances to investigate the maximum distance, which is less than the safety ranges in highway road                   |
| [45]       | I2V-V2V  | Authors investigated hybrid I2V-V2V systems, in which the car receives the signal, transmitted by the traffic light, and then re-transmitted by its rear lights to the car following it.      |
| [46]       | V2V-VLC  | The authors only study a forward connection and describe the distance over a longer distance, but still under certain unrealistic parameters  |
| [47], [48] | V2V-VLC  | Attempt experimental studies on multi-hop V2V-VLC systems, nevertheless none of these studies have derived the maximum achievable distance  |

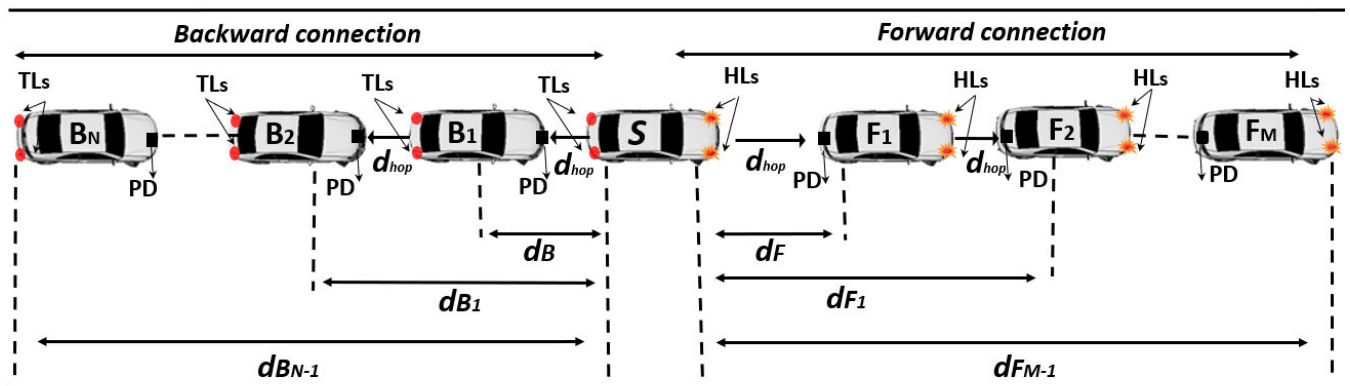


FIGURE 1. Bidirectional multi-hop V2V-VLC system in a platooning scenario.

A. CONTRIBUTIONS AND MOTIVATION

It is noticeable from the previous discussion in Section II, where the most relevant literature is listed in Table 1, that the existing literature works on V2V-VLC systems focused on individual V2V links. At the same time, most of them considered some unrealistic parameters. For instance, the ideal Lambertian profile for the vehicle’s HLs was considered in [42] and [43], which does not reflect the actual vehicle’s HLs or TLs [15], [33]. Also, in [44], the authors considered a channel path loss model that works only for shorter distances (up to 20 m) to investigate the maximum distance, less than the safety ranges in highway roads. Therefore, in this manuscript, we aim to fill this research by introducing a comprehensive study and analysis of a bidirectional multi-hop V2V-VLC system. We consider that the source vehicle communicates in two directions, i.e., Forward (F) and Backward (B). In the F link, the source vehicle (S) deploys its headlights (HLs) as wireless transmitters, while the preceding vehicle is equipped with a photodetector (PD) to receive the signal. In the B link, S utilizes its taillights (TLs) to act as the transmitters while

the vehicle in behind is equipped with another PD to receive the signal. We derive a novel closed-form expression for the maximum achievable range while satisfying a targeted bit error rate (BER) value. Our study relies on realistic channel models for both F and B links that depend on the advanced features of the ray tracing approach validated in [30], [38], and [51]. Furthermore, we investigate the effect of different system parameters on the system reliability and maximum achievable range. These parameters include system bandwidth, transmit power budget and the number of relays. Such a comprehensive study and analysis had not been previously explored in the literature, which offers valuable insights for estimating the system performance and connectivity range of bidirectional multi-hop V2V-VLC system prior to the design stage. In summary, this manuscript considers the bidirectional V2V-VLC system with realistic system and channel modelling for both F and B links and answers several critical questions that remain open in the literature, including:

- i) What is the reliable communication range that V2V VLC technology can support?

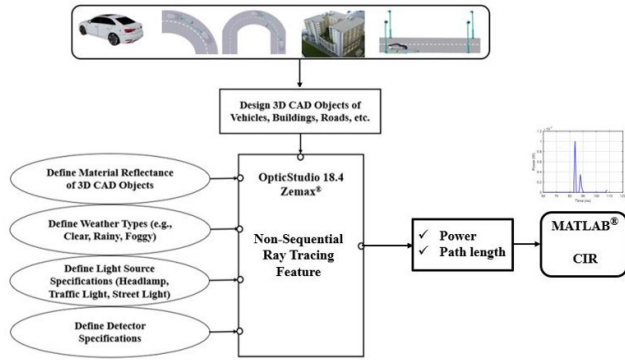


FIGURE 2. Steps required in the ray-tracing channel modeling process.

ii) How can this range be extended?

iii) What is the budget required to achieve this reliable communication range?

iv) How does the communication speed affect this range?

The remainder of this paper is organized as follows. In Section II, we describe the multi-hop V2V-VLC and channel models. Section III presents the performance analysis. Section IV presents and discusses the simulation results. Finally, Section V concludes the paper.

### III. BIDIRECTIONAL MULTI-HOP V2V-VLC SYSTEM AND CHANNEL MODEL

#### A. SYSTEM MODEL

As shown in Fig. 1, we consider a bidirectional multi-hop V2V-VLC platooning system deployed on a highway road where the source vehicle communicates in two directions, i.e., Forward (F) and Backward (B) as two distinct links with different transceivers for each one. In the Forward link, the source vehicle (S) deploys its headlights (HLs) as wireless transmitters. In contrast, the preceding vehicle (destination vehicle) is equipped with a photodetector (PD) to receive the signal. In the Backward link, however, S utilizes its taillights (TLs) to act as the transmitters. At the same time, the vehicle behind (destination vehicle in this case) is equipped with another PD to receive the signal. Forming a bidirectional link with  $M$  relay cars in the forward direction and  $N$  relay cars in the backward direction. We further define  $d_{B_{N-1}}$  and  $d_{F_{M-1}}$  as the distances between S and the destination car for the backward and forward links, respectively. In order to maintain connectivity in the platoon, the intermediate cars will act as relay nodes, which decode the signal and re-transmit it to the following vehicles (i.e., the Decode and Forward relay technique). These relay cars are separated from each other by a distance of  $d_{hop}$ . Each of the HLs or TLs has an electrical-to-optical conversion ratio of  $\eta$ , and an electrical transmission power of  $P_r$ . On the other hand, a single PD is installed in the car's rear (i.e., for the forward connection) and front (i.e., for the backward connection). It has a responsivity of  $R_p$  and an aperture diameter of  $D_r$ . Time-division duplexing (TDD) or Frequency-division duplexing (FDD) techniques can be used to mitigate self-interference in such a bidirectional V2V-VLC

system. TDD involves dividing the time slots for transmission and reception between the source and destination vehicles. During one time slot, the source vehicle's headlights (HLs) emit VLC signals received by the PD in the front vehicle (F link). In the next time slot, for communication in the opposite direction, the destination vehicle's taillights (TLs) emit VLC signals received by the PD in the source vehicle (B link). By strictly separating these time intervals, self-interference between the HLs and TLs can be mitigated. In addition, FDD can be implemented by allocating different frequency bands for transmission and reception. One frequency band can be used for HLs' VLC transmission and the front vehicle's reception, while another can be assigned for TLs' VLC transmission and the associated PD for reception. This allocation further minimizes self-interference between the HLs and TLs.

#### B. CHANNEL MODELING METHODOLOGY

The channel modelling in our work is based on the utilization of the non-sequential ray-tracing method, which was first considered for developing indoor VLC channels [52] and then applied to outdoor environment [16], [30]. As illustrated in Fig. 2, a 3D simulation platform with CAD models of cars and roads is built in OpticStudio software. Then, the surface coating material of the CAD object is defined, as well as the HL and TL features, such as their orientations, radiation patterns, and optical power. The detector's characteristics are also specified, including the aperture diameter, orientation, and field of view angle. After building the 3D platform, the non-sequential ray tracing model is performed in OpticStudio to generate an output file containing each ray's power and path length that reaches the receiver. MATLAB tools then utilize these statistics to obtain the channel impulse response (CIR).

Consider  $j \in \{B, F\}$  denoting for the backward (i.e.,  $j = B$ ) and the forward (i.e.,  $j = F$ ) directions. We then define  $K_j$  as the total number of rays associated with the  $j$ -th direction and reaching the PD. Hence,  $P_{i,j}$  and  $\tau_{i,j}$  are the corresponding optical power and propagation time of the  $i^{th}$  ray of the  $j$ -th direction, respectively. Finally, let  $\delta$  denote the Dirac delta function; the CIR can then be calculated as follows [53]:

$$H_j(t) = \sum_{i=1}^{K_j} P_{i,j} \delta(t - \tau_{i,j}). \quad (1)$$

The channel DC gain (in linear scale) of the backward V2V-VLC system (where the transmitter is the vehicle's TLs) and the forward V2V-VLC system (where the transmitter is the vehicle's HLs) can then be given by

$$h_j = \int_0^{\infty} H_j(t) dt = \begin{cases} h_B, & j = B, \text{ Backward direction.} \\ h_F, & j = F, \text{ Forward direction.} \end{cases} \quad (2)$$



Based on the ray tracing approach,  $h_B$  and  $h_F$  are given respectively by [54] and [55]

$$h_B = 10^{\left[ \frac{Pl_0}{10} + \log_{10}(d_B^{-2\alpha_b}) - \frac{\beta_b}{10} d_B \right]} \exp(-cd_B), \quad (3)$$

$$h_F = \left( \frac{D_r}{\alpha_f d_F} \right)^2 \exp(-cd_F), \quad (4)$$

where  $Pl_0$  is the reference path loss PL at  $d_0 = 1$  m, and  $d_j$  is the separation distance between the two cars, where  $j \in \{B, F\}$ . The values of  $\alpha_b$  and  $\beta_b$  correspond to 0.801 and 0.072, respectively, assuming the Audi car model [54]. In addition,  $\alpha_f$  is the correction coefficient, which is given as  $\alpha_f = 0.1585$  for clear weather conditions [30]. Thus,  $c$  represents the extinction factor for a specific weather type, and  $D_r$  is the receiver aperture size.

#### IV. PERFORMANCE ANALYSIS

As the communication distance at an acceptable bit error rate (BER) is essential for designing a multi-hop relay vehicular network scenario, this section will therefore focus on analyzing the performance of the V2V-VLC system and the communication range for a bidirectional direction that satisfies a threshold BER value.

##### A. DIRECT LINKS (FORWARD AND BACKWARD)

In this case, a direct link between the source (S) and the destination exists, the BER ( $P_e$ ) for the non-return to zero with ON-OFF keying (NRZ-OOK) modulation scheme is given by [56]

$$P_{e_j} = \frac{1}{2} \operatorname{erfc} \left( \frac{\sqrt{\gamma_j}}{2\sqrt{2}} \right), \quad (5)$$

where  $\operatorname{erfc}(x) = \frac{2}{\sqrt{\pi}} \int_x^\infty e^{-t^2} dt$  is the complementary error function and  $\gamma_j$  is the signal-to-noise ratio (SNR) of  $j^{\text{th}}$  direction, and is given by [57]

$$\gamma_j = \frac{(\eta R_p h_j)^2 P_t}{N_0 B}, \quad (6)$$

where  $B$  is the system bandwidth and  $N_0$  is the noise power spectral density. By substituting from (6) in (5), we obtain the

BER ( $P_{e_j}$ ) of  $j^{\text{th}}$  direction as

$$P_{e_j} = \frac{1}{2} \operatorname{erfc} \left( \frac{\sqrt{\frac{(\eta R_p h_j)^2 P_t}{N_0 B}}}{2\sqrt{2}} \right) \quad (7)$$

Then, the channel gain  $h_j$  for  $j \in \{B, F\}$  is obtained as follows.

$$h_j = 2\sqrt{2} \left( \sqrt{\frac{N_0 B}{P_t \eta^2 R_p^2}} \operatorname{erfc}^{-1}(2P_{e_j}) \right) \quad (8)$$

By solving (8) and (3), the total range ( $d_B$ ) for the direct backward link under the constraint of achieving a threshold BER of  $P_e^{\text{th}}$  is given by (9), as shown at the bottom of the page.

Similarly, solving equations (8) and (4) gives a total range ( $d_F$ ) for the direct forward link while still achieving a predefined  $P_e^{\text{th}}$ . This communication distance is described in (10), as shown at the bottom of the page. In (9) and (10),  $W(xe^x) = x$  denotes the Lambert wave function.

##### B. UNIDIRECTIONAL MULTI-HOP LINK

In this multi-hop vehicular network, a platooning scenario is considered where the cars are in line with the same distance between two consecutive vehicles. Assuming that the settings for the transmitters and receivers in each car are identical and applying a decode-and-forward relay mechanism for the hops, the end-to-end BER after  $n$  relays has an upper bound given by [58] and [59]

$$P_e \leq \left[ 1 - (1 - P_{eH})^{n+1} \right] \quad (11)$$

where  $n \in \{N, M\}$  is the number of hops.  $P_{eH}$  is the BER (for a specific B/F connection) occurring at each hop in this relaying mechanism, which can be approximated for the platoon scenario under consideration by [44]

$$P_{eH} \approx \frac{P_e}{n+1} \quad (12)$$

From (12) and (9), the total communication distance that satisfies a predefined  $P_e^{\text{th}}$  for the backward multi-hop link can be upper bounded by (13), as shown at the bottom of the next page.

Similarly, from (12) and (10), the upper bound for total communication distance that satisfies a predefined  $P_e^{\text{th}}$  in the forward multi-hop case is obtained using (14), as shown at the bottom of the next page.

$$d_B = \frac{20 \log_{10} e}{c \beta_b / \alpha_b} W \left[ \frac{c \beta_b / \alpha_b}{20 \log_{10} e} \exp \left( \frac{Pl_0}{10} - \log_{10} \left( 2\sqrt{2} \left( \sqrt{\frac{N_0 B}{P_t \eta^2 R_p^2}} \operatorname{erfc}^{-1}(2P_e^{\text{th}}) \right) \right) \right) \right] \quad (9)$$

$$d_F = \frac{\frac{c}{2} \left( \frac{D_r}{\alpha_f} \right) \left( 2\sqrt{2} \left( \sqrt{\frac{N_0 B}{P_t \eta^2 R_p^2}} \operatorname{erfc}^{-1}(2P_e^{\text{th}}) \right) \right)^{\frac{1}{2}}}{\frac{c}{2}} \quad (10)$$

**C. BIDIRECTIONAL LINK**

The bidirectional link represents the total range that can be achieved considering both backward and forward directions. This is given for the direct link case by summing the achievable communication distances  $d_B$  and  $d_F$  shown in (9) and (10), respectively, and for the multi-hop case by summing the achievable distances  $d_{F_M}$  and  $d_{B_N}$  derived in (13) and (14), respectively. Mathematically, the overall bidirectional ranges for the direct and multi-hop links are as follows.

$$d_T = \begin{cases} d_B + d_F, & \text{Direct link.} \\ d_{B_N} + d_{F_M}, & \text{Multi-hop link.} \end{cases} \quad (15)$$

**V. NUMERICAL RESULTS AND DISCUSSIONS**

This section presents the numerical results for the total communication ranges between the source and destination cars. Our analysis focuses on maintaining data communication within a specified BER threshold, even when the information is continuously relayed through intermediate cars. We consider three distinct links in the multi-hop V2V-VLC system: **a)** Only the backward link, **b)** Only the forward link, and **c)** Both the forward and backward links (bidirectional). Furthermore, we investigate the impact of various factors on the BER performance of both the direct and multi-hop links. These include the effect of the communication bandwidth ( $B$ ), the transmitting power ( $P_t$ ), and the number of relays for each direction ( $N$  for the backward and  $M$  for the forward directions).

**A. SIMULATION PARAMETERS**

For simulation and analysis, following conditions were considered for both transmitter and receiver, which include  $R_p = 0.28$  A/W,  $D_r = 1$  cm,  $\eta = 0.5$  W/A,  $N_0 = 10^{-21}$  W/Hz,  $P_e^{th} = 10^{-6}$ . The weather in the simulations can be considered as clear weather ( $c \approx 0$ ) thanks to the short distance between the vehicles. In addition, for the transmitting power ( $P_t$ ), these values of 10 dBm, 20 dBm, and 30 dBm are considered for analysis. Moreover, different bandwidths ( $B$ ) at 500 kHz, 1 MHz, and 2 MHz were chosen, representing the low, medium and high data rate demands in vehicular communications. Table 2 lists all parameters and their values used in the simulations.

**TABLE 2. Simulation parameters.**

|                               |  |  |
|-------------------------------|--|--|
| <b>Transmitter Parameters</b> | $\alpha_b$   | 0.801 [54]                               |
|                               | $\beta_b$  | 0.072 [54]                               |
|                               | $\alpha_f$   | 0.1585 [30]                              |
|                               | Electrical-to-Optical conversion factor ( $\eta$ ) | 0.5 (W/A)                                |
|                               | Electrical transmission power ( $P_t$ )            | 10 dBm, 20 dBm, and 30 dBm               |
| <b>Receiver Parameters</b>    | Aperture diameter ( $D_r$ )                        | 1 cm                                     |
|                               | Responsivity ( $R_p$ )                             | 0.28 (A/W)                               |
|                               | Noise power density ( $N_0$ )                      | $1 \times 10^{-21}$ (A <sup>2</sup> /Hz) |
|                               | Bandwidth ( $B$ )                                  | 500 kHz, 1 MHz, and 2 MHz                |

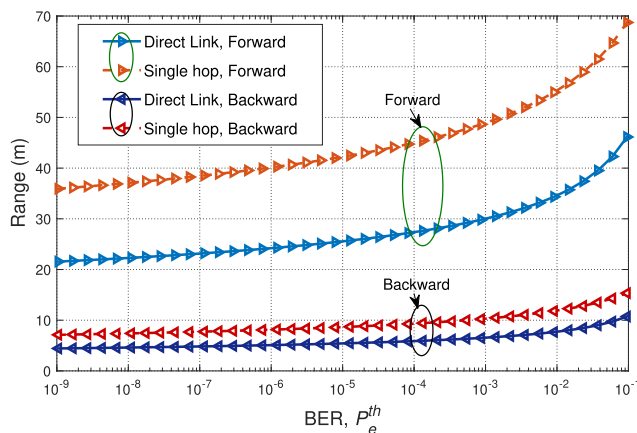


**FIGURE 3. Comparison of the total range between the direct and the single-hop systems for forward and backward links, considering  $B = 1$  MHz, and  $P_t = 20$  dBm.**

**B. UNIDIRECTIONAL LINK**

In Fig. 3, we compare the total communication range achieved in the forward and backward links, considering two different communication methods - direct and multi-hop

$$d_{B_N} \lesssim (N + 1) \frac{20 \log_{10} e}{c \beta_b / \alpha_b} W \left[ \frac{c \beta_b / \alpha_b}{20 \log_{10} e} \exp \left( \frac{\frac{P_{l_0}}{10} - \log_{10} \left( 2\sqrt{2} \left( \sqrt{\frac{N_0 B (N+1)}{P_t \eta^2 R_p^2}} \right) \operatorname{erfc}^{-1} \left( \frac{2P_e^{th}}{N+1} \right) \right)}{2\alpha_b \log_{10} e} \right) \right] \quad (13)$$

$$d_{F_M} \lesssim (M + 1) \left[ \frac{W \left( \frac{c}{2} \left( \frac{D_r}{\alpha_f} \right) \left( 2\sqrt{2} \left( \sqrt{\frac{N_0 B (M+1)}{P_t \eta^2 R_p^2}} \right) \operatorname{erfc}^{-1} \left( \frac{2P_e^{th}}{M+1} \right) \right)^{\left(\frac{1}{2}\right)}}{\frac{c}{2}} \right) \right] \quad (14)$$

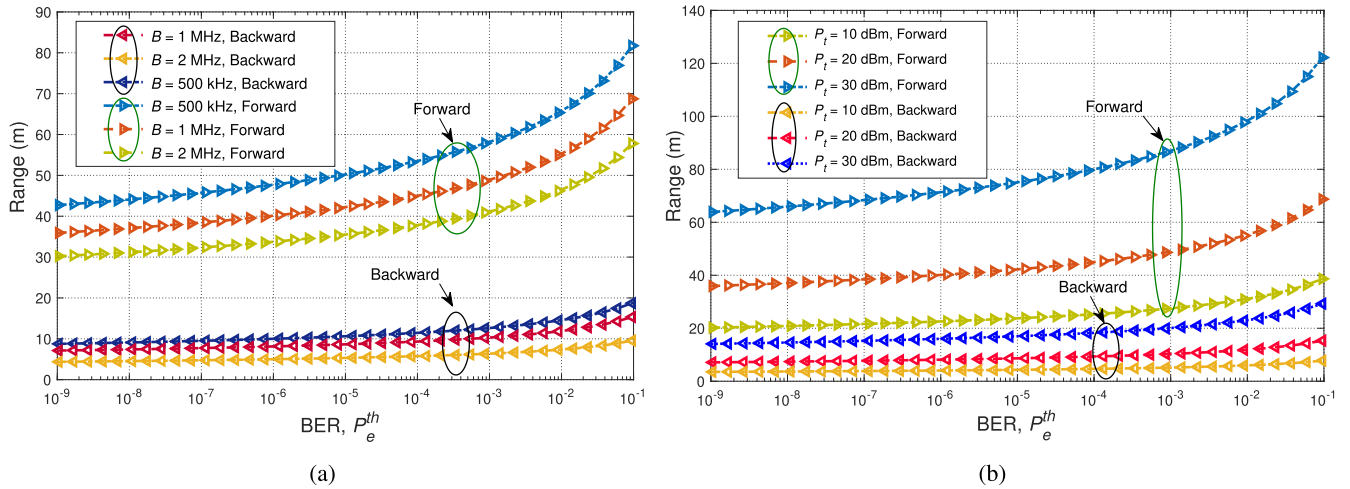


**FIGURE 4.** Achievable range versus target BER for single-hop link under the effect of (a) Bandwidth assuming  $P_t = 20$  dBm, (b) Transmit power considering  $B = 1$  MHz.

communication. In this analysis, we consider  $B = 1$  MHz,  $P_t = 20$  dBm, and a single relay ( $N = M = 1$ ). Fig. 3 demonstrates a significant enhancement in the communication range when employing multi-hop transmissions, either for the forward or the backward links, compared to a direct link. For example, we consider the backward link and a target BER of  $P_e^{th} = 10^{-6}$ . The total connectivity range at a single hop relay is  $d_{B_N} = 8$  m, which is greater than that of the direct link by 3 meters. Similarly, for the forward direction, the total communication range  $d_{F_M}$  reaches 40 meters for the single relay, which is more significant than  $d_F$  (direct link) by 16 meters. Consequently, an extension in the communication range for the bidirectional one-hop relay system will be up to 19 meters. In other words, by deploying only a single relay, the proposed VLC system has provided an enhancement of 37.5% in the case of the backward link. This improvement becomes more significant when applying for the forward link (at more than 40%). Thus, it is clear that deploying a multi-hop relay system is an alternative solution that can compensate for the range decay.

In Fig. 3, we compare the total communication range achieved in the forward and backward links, considering two different communication methods - direct and multi-hop communication. In this analysis, we consider  $B = 1$  MHz,  $P_t = 20$  dBm, and a single relay ( $N = M = 1$ ). Fig. 3 demonstrates a significant enhancement in the communication range when employing multi-hop transmissions, either for the forward or the backward links, compared to a direct link. For example, we consider the backward link and a target BER of  $P_e^{th} = 10^{-6}$ . The total connectivity range at a single hop relay is  $d_{B_N} = 8$  m, greater than the direct link by 3 meters. Similarly, for the forward direction, the total communication range  $d_{F_M}$  reaches 40 meters for the single relay, which is more significant than  $d_F$  (direct link) by 16 meters. Consequently, an extension in the communication range for the bidirectional one-hop relay system will be up to

19 meters. In other words, by deploying only a single relay, the proposed VLC system has provided an enhancement of 37.5% in the case of the backward link. This improvement becomes more significant when applying for the forward link (at more than 40%). Thus, it is clear that deploying a multi-hop relay system is an alternative solution that can compensate for the range decay.

In Fig. 4.a, we consider the unidirectional single-hop links separately, which include a forward link and a backward link, and investigate the effect of the bandwidth on the total range that can be reached while achieving the target BER level. We consider a transmit power of  $P_t = 20$  dBm. The results showed a remarkable impact of the system bandwidth on the total range for both forward and backward links. A higher bandwidth leads to a higher noise variance, resulting in a lower SNR and, thus, a reduced communication range. As an example, consider a threshold BER of  $P_e^{th} = 10^{-6}$  and the backward link. The total communication range assuming  $B = 2$  MHz is given by  $d_{B_N} \approx 6$  m. This value climbs to 8 m and 10 m for  $B = 1$  MHz and  $B = 500$  kHz, respectively. Similarly, consider  $P_e^{th} = 10^{-6}$  and the forward link. The total attainable range is given as  $d_{F_M} = 32$  m,  $d_{F_M} = 40$  m, and  $d_{F_M} = 49$  m for  $B = 2$  MHz,  $B = 1$  MHz, and  $B = 500$  kHz, respectively. One can notice that the total communication ranges are different for backward and forward links. In other words, the total range using the HLs transmitters (forward link) is higher than that achieved using the TLs transmitters (backward link) with an approximately quintuple. This difference can be attributed to the higher intensity profile of HL lamps than TLs, which is related to their distinct working purposes. For example, consider  $B = 1$  MHz, the total range is given as  $d_{B_N} = 8$  m for the backward link and as  $d_{F_M} = 40$  m for the forward one, i.e.,  $d_{F_M} = 5 d_{B_N}$ .

In Fig. 4.b, we consider the unidirectional single-hop links separately and investigate the effect of electrical transmit power on the total range for each link. We consider

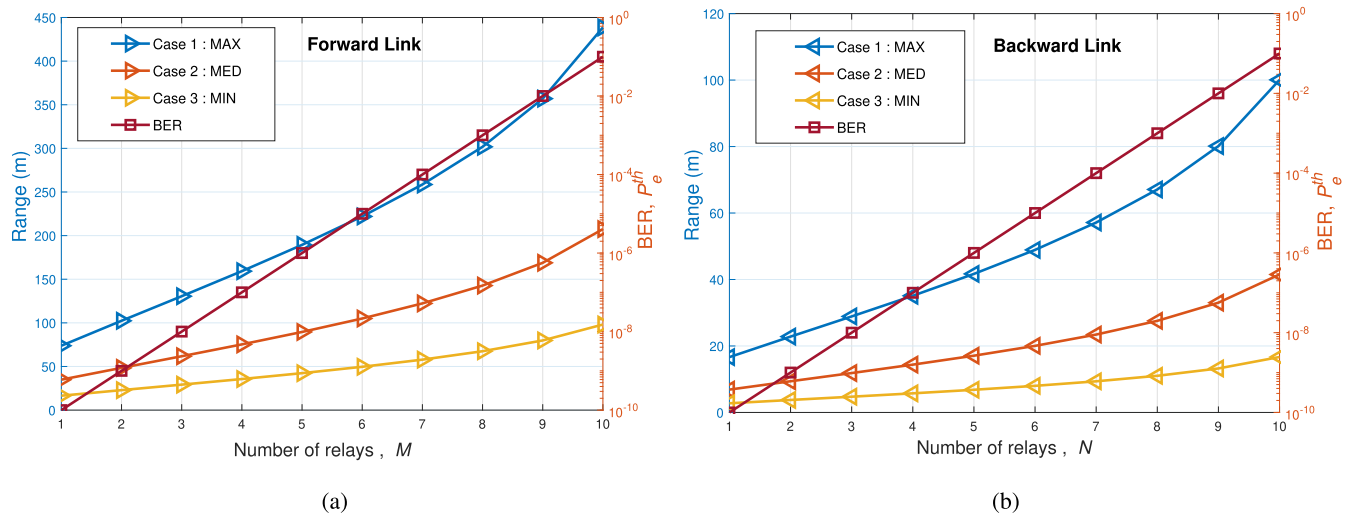


**FIGURE 5.** Total range for multi-hop system versus a target of BER at different electrical transmit power budgets and different values of bandwidth, for the Forward (a) and Backward (b) links at  $N, M \in \{1, 2, \dots, 10\}$ .

$B = 1$  MHz and  $P_e^{th} = 10^{-6}$ . The simulation results show that the transmit power budget significantly influences the communication range, with a varying effect between the backward and forward links. For example, consider  $P_t = 30$  dBm (unity power). The total ranges for the backward and forward links are  $d_{B_N} = 17$  m and  $d_{F_M} = 71$  m, respectively. When the power budget is reduced to  $P_t = 20$  dBm, the total range for the backward link drops by 9 m or 50% (i.e.,  $d_{B_N} \approx 8$  m), whereas the total range for the forward link decreases by 31 m or 40% (i.e.,  $d_{F_M} \approx 40$  m).

In Fig. 5, we analyze the impact of different cases on the communication range and BER for unidirectional multi-hop links. We consider three cases: MAX, MED, and MIN, each with specific parameter settings as follows:

i) **Case 1: MAX** is for the case achieved when  $B = 500$  KHz and  $P_t = 30$  dBm.

ii) **Case 2: MED** is for the case achieved when  $B = 1$  MHz,  $P_t = 20$  dBm.

iii) **Case 3: MIN** is for the case achieved when  $B = 2$  MHz,  $P_t = 10$  dBm.

In Fig. 5.a and Fig. 5.b, we investigate the impact of increasing the number of relays on the total communication range and BER performance for both forward and backward links. An increasing number of relays increases the total communication range for both the forward (Fig. 5.a) and backward (Fig. 5.b) links. For example, consider  $N = M = 3$  and Case 1. The total ranges for the forward and backward links are  $d_{F_M} = 140$  m and  $d_{B_N} = 29$  m, respectively. When the number of relays reduces (i.e.,  $N = M = 1$ ), the total range decreases for the forward link by 70 m or by 51% (i.e.,  $d_{F_M} \approx 65$  m) and for the backward one by 11 m or by 37.9% (i.e.,  $d_{B_N} = 18$  m). Nevertheless, it is crucial to acknowledge that this expansion in communication range comes at the expense of a decline in communication quality. This degradation is due to the introduction of additional hops as the number of relays

increases, which leads to higher levels of interference, signal attenuation, and potential transmission errors. For instance, consider  $N = M = 4$  and Case 2, the BER reached for the forward and backward links is set to  $8 \times 10^{-8}$  and  $9 \times 10^{-8}$ , respectively. However, as the number of relays increases to  $N = M = 8$ , the BER deteriorates to  $7 \times 10^{-7}$  and  $5 \times 10^{-7}$  for the forward and backward links, respectively. Therefore, a careful trade-off must be made between extending the range and maintaining satisfactory communication quality.

Table 3 comprehensively summarizes the bidirectional and unidirectional total ranges for forward and backward links across different cases and relay numbers. The table considers the cases applied with equal relays for both directions ( $N = M$ ) and offers valuable insights into the relationship between the number of relays, signal quality, electrical transmit power, bandwidth, and communication range. The analysis indicates that the total communication range expands with an increasing number of relays; however, this expansion is accompanied by a reduction in signal quality. One potential solution to this trade-off is to decrease the bandwidth and increase the transmitted power. Such adjustments can improve the signal quality and maintain an acceptable level of communication range. For example, consider  $N = M = 5$  and  $P_e^{th} = 10^{-6}$ , and the forward link. The range achieved is  $d_{F_M} = 190$  m for the MAX case. However, this range diminishes to  $d_{F_M} = 90$  m and  $d_{F_M} = 45$  m for the MED and MIN cases, respectively. Similarly, focusing on the backward link, the achieved range is  $d_{B_N} = 40$  m for the MAX case. This reduces to  $d_{B_N} = 17$  m and  $d_{B_N} = 7$  m for the MED and MIN cases, respectively. Likewise, for the bidirectional link, the ranges obtained are  $d_T = 230$  m, 107 m, and 52 m, respectively, for the MAX, MED, and MIN cases.

In Fig. 6, we consider unidirectional single-hop links and investigate the effect of electrical transmit power on the total range for both forward (Fig. 6.a) and backward (Fig. 6.b)



TABLE 3. Achievable range for unidirectional and bidirectional multi-hop for the case  $N = M \in \{5, 6, 7\}$ .

| Cases<br>BER | MAX<br>500 KHz, 30 dBm |           |           | MED<br>1 MHz, 20 dBm |           |           | MIN<br>2 MHz, 10 dBm |           |           |
|--------------|------------------------|-----------|-----------|----------------------|-----------|-----------|----------------------|-----------|-----------|
|              | $10^{-6}$              | $10^{-5}$ | $10^{-4}$ | $10^{-6}$            | $10^{-5}$ | $10^{-4}$ | $10^{-6}$            | $10^{-5}$ | $10^{-4}$ |
| $M$          | 5                      | 6         | 7         | 5                    | 6         | 7         | 5                    | 6         | 7         |
| $N$          | 5                      | 6         | 7         | 5                    | 6         | 7         | 5                    | 6         | 7         |
| $d_{FM}$ (m) | 190                    | 225       | 260       | 90                   | 102       | 125       | 45                   | 50        | 55        |
| $d_{BN}$ (m) | 40                     | 50        | 55        | 17                   | 20        | 24        | 7                    | 8         | 10        |
| $d_T$ (m)    | 230                    | 275       | 315       | 107                  | 122       | 149       | 52                   | 58        | 65        |

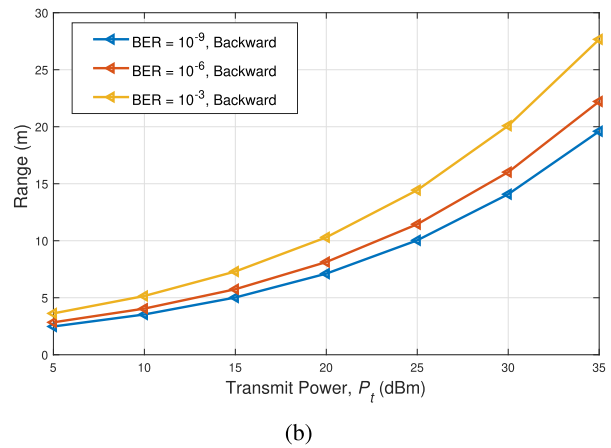
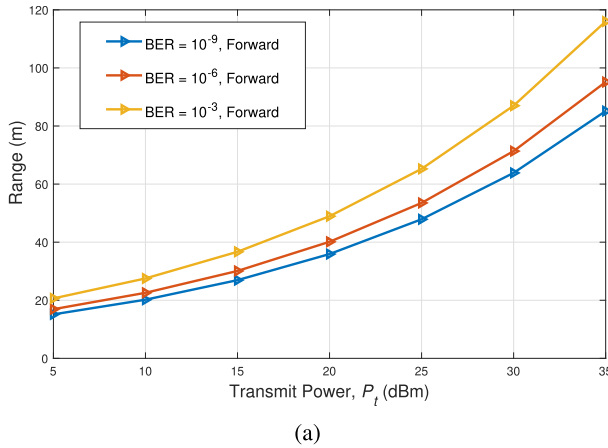


FIGURE 6. Total range for single-hop system versus the transmit power at different values of BER, for (a) Forward and (b) Backward link, considering  $B = 1$  MHz.

links. It is observed that when the electrical transmit power increases, the total communication range increases for both forward and backward links. For example, consider a target BER of  $P_e = 10^{-6}$ ,  $B = 1$  MHz, and  $P_t = 15$  dBm. The total communication range is set to  $d_{FM} = 30$  m and  $d_{BN} = 6.5$  m for forward and backward links, respectively. As the electrical transmit power is increased to 20 dBm, these ranges escalate to  $d_{FM} = 40$  m and  $d_{BN} = 8$  m. Furthermore, the ranges further expand to  $d_{FM} = 75$  m and  $d_{BN} = 16$  m for  $P_t = 30$  dBm.

C. BIDIRECTIONAL LINK

Fig. 7 shows the range of the bidirectional multi-hop relay system with different deployment scenarios illustrated as follows:

i) **Scenario 1:** This is the benchmark scenario in which a bidirectional direct system is considered (i.e.,  $N = M = 0$  or  $d_T = d_B + d_F$ ).

ii) **Scenario 2:** We consider a multi-hop bidirectional system with  $N = M = 1$ .

iii) **Scenario 3:** We consider a multi-hop bidirectional system with  $N = M/2 = 1$ .

iv) **Scenario 4:** This is a reverse of the previous scenario where  $M = N/2 = 1$ .

We further consider a target BER of  $P_e^{th} = 10^{-6}$ ,  $B = 1$  MHz, and  $P_t = 20$  dBm. It is observed that increasing  $N$

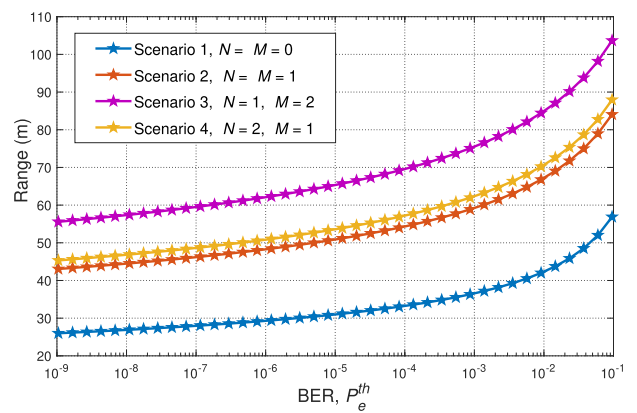
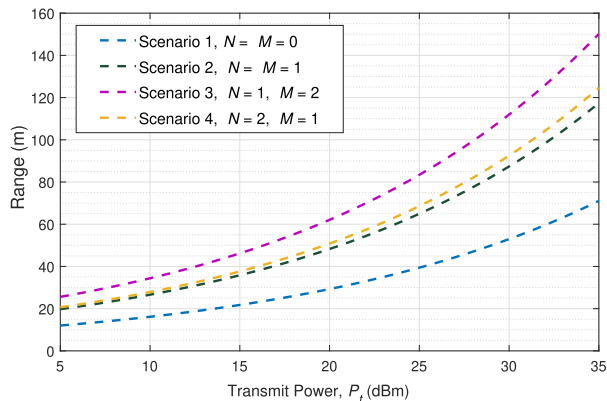


FIGURE 7. The range of bidirectional multi-hop relay system at different deployment scenarios, considering  $B = 1$  MHz, and  $P_t = 20$  dBm.

or  $M$  (i.e., Scenarios 2, 3, and 4) enlarges the communication range for the benchmark scenario (i.e., Scenario 1). However, one can observe that Scenario 3 provides the largest communication range, which is achieved when the number of relays of the front link is greater than that of the backlink, i.e.,  $M > N$ . For example, the total ranges are given for scenarios 1, 2, 3, and 4 as  $d_T = 30$  m, 49 m, 51 m, and 63 m, respectively.

Fig. 8 shows the bidirectional multi-hop relay system range with different deployment scenarios versus the electrical



**FIGURE 8.** The range of bidirectional multi-hop relay system at different deployment scenarios, considering  $B = 1$  MHz,  $P_e^{th} = 10^{-6}$ , and  $P_t = 20$  dBm.

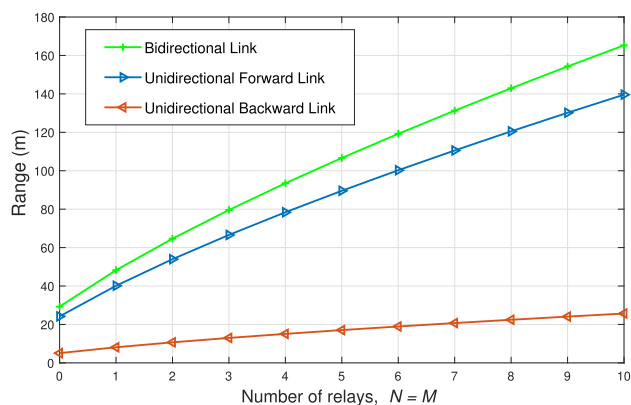


**FIGURE 9.** The range of bidirectional multi-hop relay system at different number of relays, considering  $B = 1$  MHz,  $P_e^{th} = 10^{-6}$ , and  $P_t = 20$  dBm.

transmit power  $P_t$ . The observed results showed that increasing the transmit power enlarges the communication range for all scenarios (i.e., Scenarios 2, 3, and 4) concerning the benchmark scenario (i.e., Scenario 1). For instance, consider  $P_e^{th} = 10^{-6}$ ,  $B = 1$  MHz, and  $P_t = 10$  dBm. The ranges for scenarios 1, 2, 3, and 4 are  $d_T = 19$  m, 24 m, 26 m, and 39 m, respectively. This value increases to  $d_T = 59$  m, 82 m, 91 m, and 117 m, respectively, for  $P_t = 30$  dBm.

This study demonstrates the advantages of implementing a bidirectional multi-hop relaying on the VVLC system. In Fig. 9, we consider case 2 ( $B = 1$  MHz,  $P_t = 20$  dBm) and investigate the effect of increasing the relay number on the communication range for bidirectional and unidirectional links. We consider  $N = M$ , and  $P_e^{th} = 10^{-6}$ . It is observed that the total range increases with an increase in the number of intermediate relays. For example, consider  $M = N = 2$ ; the total range is given for the bidirectional link as  $d_T = 62$  m. This climbs to  $d_T = 94$  m and to  $d_T = 143$  m for  $M = N = 4$ , and  $M = N = 8$ , respectively. Furthermore, it is worth noting that the bidirectional link exhibits the greatest communication range compared to the unidirectional links, either in the forward or backward direction. This observation highlights the advantage of bidirectional communication in

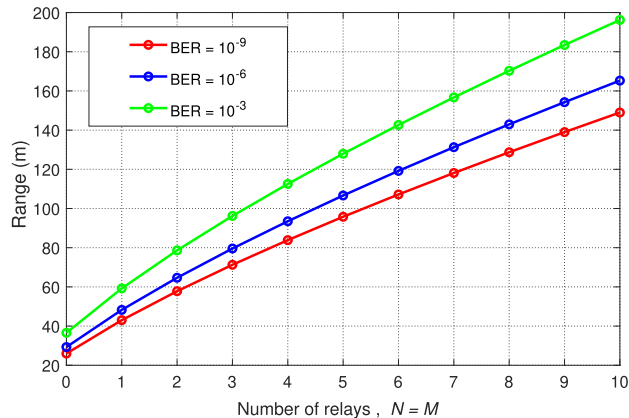


**FIGURE 10.** The range of bidirectional multi-hop relay system versus number of relays at different target of BER, assuming  $N = M$ ,  $B = 1$  MHz and  $P_t = 20$  dBm.

extending communication reach and enhancing the coverage and connectivity in VVLC systems. For instance, when  $M = N = 1$ , the achieved ranges for the bidirectional link, unidirectional forward link, and unidirectional backward link are given by  $d_T = 48$  m,  $d_{FM} = 40$  m, and  $d_{BN} = 8$  m, respectively. It should be noted that using one relay for the bidirectional link can enhance the communication range by more than 19 m (i.e.,  $d_T \approx 29$  m for  $M = N = 0$ ).

In Fig. 10, we consider specific BER targets and present the bidirectional communication range that can be reached versus the relay numbers. We assume Scenario 1 ( $N = M$ ),  $B = 1$  MHz,  $P_t = 20$  dBm, and different target BER (i.e.,  $P_e^{th} = 10^{-9}$ ,  $P_e^{th} = 10^{-6}$ , and  $P_e^{th} = 10^{-3}$ ). It is observed that the total bidirectional range increases with an increase in the number of intermediate relays. For example, consider  $P_e^{th} = 10^{-6}$ , the total range is given for  $M = N = 1$  as  $d_T = 50$  m. This climbs to  $d_T = 113$  m and  $d_T = 169$  m for  $M = N = 5$ , and  $M = N = 10$ , respectively. It is also observed that achieving a better BER target reduces the achieved bidirectional communication distance. For instance, consider  $M = N = 5$ , the ranges for  $P_e^{th} = 10^{-9}$ ,  $P_e^{th} = 10^{-6}$ , and  $P_e^{th} = 10^{-3}$  are given by  $d_T = 97$  m, 109 m, and 127 m, respectively.

## VI. CONCLUSION

In this paper, we have analyzed the performance of a bidirectional multi-hop V2V-VLC system using realistic channel models that capture the asymmetrical intensity profiles of HLs and TLs. We have derived a closed-form expression for the total communication range at a target BER. We have also investigated the impacts of the system bandwidth, transmit power budget, and number of intermediate relays on the system performance. Our analysis provides insights into the relationships between system parameters and their impact on the connectivity range for unidirectional and bidirectional communication. Our results show that the communication range is highly dependent on the transmitter type, with HLs supporting five times the communication range of TLs. We have also demonstrated that using intermediate cars

as relay nodes can extend the communication range. Our findings highlight the direct impact of the number of relays on the communication distance, indicating that increased relays can effectively enhance the range. However, careful selection of relays is essential as the communication quality may deteriorate with excessive relays. Our results further reveal that bidirectional multi-hop V2V-VLC systems significantly enhance the total communication range, with forward relays having a more significant impact than backward relays. Another critical factor in the ITSs is latency [60], which we aim to investigate in our future work, giving more insights into the minimum latency that can be achieved using VLC technology and its improvements concerning other RF technologies. Furthermore, Vehicle-to-Network (V2N) is a vital parameter in the ITSs, which could also be considered for future research. To further improve V2V communication range and data rates, VVLC can be integrated with various radio frequency connectivity enablers, such as V2X cellular communications and dedicated short-range communications, which may be considered in our future work.

## REFERENCES

- [1] S. Zeadally, M. A. Javed, and E. B. Hamida, "Vehicular communications for ITS: Standardization and challenges," *IEEE Commun. Standards Mag.*, vol. 4, no. 1, pp. 11–17, Mar. 2020.
- [2] O. Pribyl, P. Pribyl, M. Lom, and M. Svitek, "Modeling of smart cities based on ITS architecture," *IEEE Intell. Transp. Syst. Mag.*, vol. 11, no. 4, pp. 28–36, Jun. 2019.
- [3] Z. MacHardy, A. Khan, K. Obana, and S. Iwashina, "V2X access technologies: Regulation, research, and remaining challenges," *IEEE Commun. Surveys Tuts.*, vol. 20, no. 3, pp. 1858–1877, 3rd Quart., 2018.
- [4] J. B. Kenney, "Dedicated short-range communications (DSRC) standards in the United States," *Proc. IEEE*, vol. 99, no. 7, pp. 1162–1182, Jul. 2011.
- [5] K. Abboud, H. A. Omar, and W. Zhuang, "Interworking of DSRC and cellular network technologies for V2X communications: A survey," *IEEE Trans. Veh. Technol.*, vol. 65, no. 12, pp. 9457–9470, Dec. 2016.
- [6] M. M. Saad, M. T. R. Khan, S. H. A. Shah, and D. Kim, "Advancements in vehicular communication technologies: C-V2X and NR-V2X comparison," *IEEE Commun. Mag.*, vol. 59, no. 8, pp. 107–113, Aug. 2021.
- [7] Z. H. Mir, J. Toutouh, F. Filali, and Y.-B. Ko, "Enabling DSRC and C-V2X integrated hybrid vehicular networks: Architecture and protocol," *IEEE Access*, vol. 8, pp. 180909–180927, 2020.
- [8] E. Güney, C. Bayılmış, and B. Çakan, "An implementation of real-time traffic signs and road objects detection based on mobile GPU platforms," *IEEE Access*, vol. 10, pp. 86191–86203, 2022.
- [9] E. Güney, C. Bayılmış, and B. Çakan, "Corrections to 'an implementation of real-time traffic signs and road objects detection based on mobile GPU platforms,'" *IEEE Access*, vol. 10, pp. 103587–103587, 2022.
- [10] R. Molina-Masegosa and J. Gozalvez, "LTE-V for sidelink 5G V2X vehicular communications: A new 5G technology for short-range vehicle-to-everything communications," *IEEE Veh. Technol. Mag.*, vol. 12, no. 4, pp. 30–39, Dec. 2017.
- [11] L. Cheng, W. Viriyasitavat, M. Boban, and H.-M. Tsai, "Comparison of radio frequency and visible light propagation channels for vehicular communications," *IEEE Access*, vol. 6, pp. 2634–2644, 2018.
- [12] M. Uysal, Z. Ghassemlooy, A. Bekkali, A. Kadri, and H. Menouar, "Visible light communication for vehicular networking: Performance study of a V2V system using a measured headlamp beam pattern model," *IEEE Veh. Technol. Mag.*, vol. 10, no. 4, pp. 45–53, Dec. 2015.
- [13] A.-M. Cailean and M. Dimian, "Impact of IEEE 802.15.7 standard on visible light communications usage in automotive applications," *IEEE Commun. Mag.*, vol. 55, no. 4, pp. 169–175, Apr. 2017.
- [14] S. Yahia, Y. Meraihi, A. Ramdane-Cherif, A. B. Gabis, D. Acheli, and H. Guan, "A survey of channel modeling techniques for visible light communications," *J. Netw. Comput. Appl.*, vol. 194, Nov. 2021, Art. no. 103206.
- [15] A. Memedi and F. Dressler, "Vehicular visible light communications: A survey," *IEEE Commun. Surveys Tuts.*, vol. 23, no. 1, pp. 161–181, 1st Quart., 2021.
- [16] H. B. Eldeeb, S. M. Sait, and M. Uysal, "Visible light communication for connected vehicles: How to achieve the omnidirectional coverage?" *IEEE Access*, vol. 9, pp. 103885–103905, 2021.
- [17] H. Abuella, F. Miramirkhani, S. Ekin, M. Uysal, and S. Ahmed, "ViLDAR—Visible light sensing-based speed estimation using vehicle headlamps," *IEEE Trans. Veh. Technol.*, vol. 68, no. 11, pp. 10406–10417, Nov. 2019.
- [18] P. Sharda, G. S. Reddy, M. R. Bhatnagar, and Z. Ghassemlooy, "A comprehensive modeling of Vehicle-to-Vehicle based VLC system under practical considerations, an investigation of performance, and diversity property," *IEEE Trans. Commun.*, vol. 70, no. 5, pp. 3320–3332, May 2022.
- [19] H. B. Eldeeb, M. Elamassie, S. M. Sait, and M. Uysal, "Infrastructure-to-vehicle visible light communications: Channel modelling and performance analysis," *IEEE Trans. Veh. Technol.*, vol. 71, no. 3, pp. 2240–2250, Mar. 2022.
- [20] B. Turan and S. Coleri, "Machine learning based channel modeling for vehicular visible light communication," *IEEE Trans. Veh. Technol.*, vol. 70, no. 10, pp. 9659–9672, Oct. 2021.
- [21] A. Al-Kinani, C.-X. Wang, Q. Zhu, Y. Fu, E. M. Aggoune, A. Talib, and N. A. Al-Hasaani, "A 3D non-stationary GBSM for vehicular visible light communication MISO channels," *IEEE Access*, vol. 8, pp. 140333–140347, 2020.
- [22] M. A. Arfaoui, M. D. Soltani, I. Tavakkolnia, A. Ghayeb, M. Safari, C. M. Assi, and H. Haas, "Physical layer security for visible light communication systems: A survey," *IEEE Commun. Surveys Tuts.*, vol. 22, no. 3, pp. 1887–1908, 3rd Quart., 2020.
- [23] B. Turan, O. Narmanlioglu, S. C. Ergen, and M. Uysal, "Physical layer implementation of standard compliant vehicular VLC," in *Proc. IEEE 84th Veh. Technol. Conf. (VTC-Fall)*, Sep. 2016, pp. 1–5.
- [24] G. Gurbilek, M. Koca, A. Uyrus, B. Soner, E. Basar, and S. Coleri, "Location-aware adaptive physical layer design for vehicular visible light communication," in *Proc. IEEE Veh. Netw. Conf. (VNC)*, Dec. 2019, pp. 1–4.
- [25] A. Memedi, C. Sommer, and F. Dressler, "On the need for coordinated access control for vehicular visible light communication," in *Proc. 14th Annu. Conf. Wireless On-Demand Netw. Syst. Services (WONS)*, Feb. 2018, pp. 121–124.
- [26] H. B. Eldeeb, E. Yanmaz, and M. Uysal, "MAC layer performance of multi-hop vehicular VLC networks with CSMA/CA," in *Proc. 12th Int. Symp. Commun. Syst., Netw. Digit. Signal Process. (CSNDSP)*, Jul. 2020, pp. 1–6.
- [27] M. S. Demir, H. B. Eldeeb, and M. Uysal, "CoMP-based dynamic handover for vehicular VLC networks," *IEEE Commun. Lett.*, vol. 24, no. 9, pp. 2024–2028, Sep. 2020.
- [28] J. Chen and Z. Wang, "Topology control in hybrid VLC/RF vehicular ad-hoc network," *IEEE Trans. Wireless Commun.*, vol. 19, no. 3, pp. 1965–1976, Mar. 2020.
- [29] T. Ismail, M. E. Gad, and B. Mokhtar, "Integrated VLC/RF wireless technologies for reliable content caching system in vehicular networks," *IEEE Access*, vol. 9, pp. 51855–51864, 2021.
- [30] M. Karbalayghareh, F. Miramirkhani, H. B. Eldeeb, R. C. Kizilirmak, S. M. Sait, and M. Uysal, "Channel modelling and performance limits of vehicular visible light communication systems," *IEEE Trans. Veh. Technol.*, vol. 69, no. 7, pp. 6891–6901, Jul. 2020.
- [31] M. Akanegawa, Y. Tanaka, and M. Nakagawa, "Basic study on traffic information system using LED traffic lights," *IEEE Trans. Intell. Transp. Syst.*, vol. 2, no. 4, pp. 197–203, Jun. 2001.
- [32] N. Kumar, D. Terra, N. Lourenço, L. N. Alves, and R. L. Aguiar, "Visible light communication for intelligent transportation in road safety applications," in *Proc. 7th Int. Wireless Commun. Mobile Comput. Conf.*, Jul. 2011, pp. 1513–1518.
- [33] *Uniform Provisions Concerning the Approval of Motor Vehicle Headlamps Emitting an Asymmetrical Passing Beam or a Driving Beam or Both and Equipped With Filament Lamps*, Regulation no. 112, Revision 1, United Nations, New York, NY, USA, Oct. 2006.
- [34] W. Viriyasitavat, S.-H. Yu, and H.-M. Tsai, "Short paper: Channel model for visible light communications using off-the-shelf scooter taillight," in *Proc. IEEE Veh. Netw. Conf.*, Dec. 2013, pp. 170–173.



- [35] H. B. Eldeeb, E. Eso, M. Uysal, Z. Ghassemlooy, S. Zvanovec, and J. Sathian, "Vehicular visible light communications: The impact of taillight radiation pattern," in *Proc. IEEE Photon. Conf. (IPC)*, Sep. 2020, pp. 1–2.
- [36] P. Luo, Z. Ghassemlooy, H. L. Minh, E. Bentley, A. Burton, and X. Tang, "Performance analysis of a car-to-car visible light communication system," *Appl. Opt.*, vol. 54, no. 7, pp. 1696–1706, 2015.
- [37] S. Yahia, Y. Meraihi, A. Ramdane-Cherif, T. D. Ho, and H. B. Eldeeb, "Enhancement of vehicular visible light communication using spherical detector and custom lens combinations," *IEEE Access*, vol. 11, pp. 21600–21611, 2023.
- [38] B. Aly, M. Elamassie, H. B. Eldeeb, and M. Uysal, "Experimental investigation of lens combinations on the performance of vehicular VLC," in *Proc. 12th Int. Symp. Commun. Syst., Netw. Digit. Signal Process. (CSNDSP)*, Jul. 2020, pp. 1–5.
- [39] H. B. Eldeeb, S. Naser, L. Bariah, and S. Muhaidat, "Energy and spectral efficiency analysis for RIS-aided V2V-visible light communication," *IEEE Commun. Lett.*, vol. 27, no. 9, pp. 2373–2377, Mar. 2023.
- [40] M. Jerbi and S. M. Senouci, "Characterizing multi-hop communication in vehicular networks," in *Proc. IEEE Wireless Commun. Netw. Conf.*, Mar. 2008, pp. 3309–3313.
- [41] Y. Ihara, H. Kremo, O. Altintas, H. Tanaka, M. Ohtake, T. Fujii, C. Yoshimura, K. Ando, K. Tsukamoto, M. Tsuru, and Y. Oie, "Distributed autonomous multi-hop vehicle-to-vehicle communications over TV white space," in *Proc. IEEE 10th Consum. Commun. Netw. Conf. (CCNC)*, Jan. 2013, pp. 336–344.
- [42] A. Bazzi, B. M. Masini, A. Zanella, and A. Calisti, "Visible light communications in vehicular networks for cellular offloading," in *Proc. IEEE Int. Conf. Commun. Workshop (ICCW)*, Jun. 2015, pp. 1416–1421.
- [43] M. Y. Abualhou, O. Shagdar, and F. Nashashibi, "Visible light inter-vehicle communication for platooning of autonomous vehicles," in *Proc. IEEE Intell. Vehicles Symp. (IV)*, Jun. 2016, pp. 508–513.
- [44] M. Elamassie, M. Karbalayghareh, F. Miramirkhani, R. C. Kizilirmak, and M. Uysal, "Effect of fog and rain on the performance of vehicular visible light communications," in *Proc. IEEE 87th Veh. Technol. Conf. (VTC Spring)*, Jun. 2018, pp. 1–6.
- [45] H. B. Eldeeb, M. Elamassie, and M. Uysal, "Performance analysis and optimization of cascaded I2V and V2V VLC links," in *Proc. 17th Int. Sympos. Wireless Commun. Syst. (ISWCS)*, 2021, pp. 1–6.
- [46] H. B. Eldeeb, F. Miramirkhani, and M. Uysal, "A path loss model for vehicle-to-vehicle visible light communications," in *Proc. 15th Int. Conf. Telecommun. (ConTEL)*, Jul. 2019, pp. 1–5.
- [47] O. Narmanlioglu, B. Turan, S. C. Ergen, and M. Uysal, "Cooperative MIMO-OFDM based inter-vehicular visible light communication using brake lights," *Comput. Commun.*, vol. 120, pp. 138–146, May 2018.
- [48] S. Ucar, S. C. Ergen, and O. Ozkasap, "Security vulnerabilities of IEEE 802.11p and visible light communication based platoon," in *Proc. IEEE Veh. Netw. Conf. (VNC)*, Dec. 2016, pp. 1–4.
- [49] A.-M. Cailean, B. Cagneau, L. Chassagne, S. Topsu, Y. Alayli, and M. Dimian, "Visible light communications cooperative architecture for the intelligent transportation system," in *Proc. IEEE 20th Symp. Commun. Veh. Technol. Benelux (SCVT)*, Nov. 2013, pp. 1–5.
- [50] M. S. Demir, H. B. Eldeeb, and M. Uysal, "Relay-assisted handover technique for vehicular VLC networks," *ITU J. Future Evolving Technol.*, vol. 3, no. 1, pp. 11–18, 2022.
- [51] H. B. Eldeeb, S. M. Mana, V. Jungnickel, P. Hellwig, J. Hilt, and M. Uysal, "Distributed MIMO for li-fi: channel measurements, ray tracing and throughput analysis," *IEEE Photon. Technol. Lett.*, vol. 33, no. 16, pp. 916–919, Aug. 15, 2021.
- [52] Z. N. Chaleshtori, Z. Ghassemlooy, H. B. Eldeeb, M. Uysal, and S. Zvanovec, "Utilization of an OLED-based VLC system in office, corridor, and semi-open corridor environments," *Sensors*, vol. 20, no. 23, p. 6869, Dec. 2020.
- [53] E. Sarbazi, M. Uysal, M. Abdallah, and K. Qaraqe, "Ray tracing based channel modeling for visible light communications," in *Proc. 22nd Signal Process. Commun. Appl. Conf. (SIU)*, Apr. 2014, pp. 702–705.
- [54] H. B. Eldeeb, E. Eso, E. A. Jarchlo, S. Zvanovec, M. Uysal, Z. Ghassemlooy, and J. Sathian, "Vehicular VLC: A ray tracing study based on measured radiation patterns of commercial taillights," *IEEE Photon. Technol. Lett.*, vol. 33, no. 16, pp. 904–907, Aug. 15, 2021.
- [55] P. Sharda, G. S. Reddy, M. R. Bhatnagar, and Z. Ghassemlooy, "A comprehensive modeling of vehicle-to-vehicle based VLC system under practical considerations, an investigation of performance, and diversity property," *IEEE Trans. Commun.*, vol. 70, no. 5, pp. 3320–3332, May 2022.
- [56] L. C. Andrews and R. L. Phillips, *Laser Beam Propagation Through Random Media*, vol. 1, 2nd ed. Bellingham, WA, USA: SPIE, Sep. 2005.
- [57] Z. Ghassemlooy, W. Popoola, and S. Rajbhandari, *Optical Wireless Communications: System and Channel Modelling With MATLAB®*. Boca Raton, FL, USA: CRC Press, 2019.
- [58] T. S. Rappaport, "Wireless communications—principles and practice, (the book end)," *Microw. J.*, vol. 45, no. 12, pp. 128–129, 2002.
- [59] A. Florea and H. Yanikomeroglu, "On the optimal number of hops in infrastructure-based fixed relay networks," in *Proc. IEEE Global Telecommun. Conf. (GLOBECOM)*, Jul. 2005, pp. 3242–3247.
- [60] S. Caputo, L. Mucchi, M. A. Umair, M. Meucci, M. Seminara, and J. Catani, "The role of bidirectional VLC systems in low-latency 6G vehicular networks and comparison with IEEE802.11p and LTE/5G C-V2X," *Sensors*, vol. 22, no. 22, p. 8618, Nov. 2022.



**SOUAD REFAS** received the B.Sc. and M.Sc. degrees in networks and telecommunications from the Department of Electrical Engineering, University of M'Hamed Bougara Boumerdes, Algeria, in 2018 and 2020, respectively. During her M.Sc., she was studying optical wireless communications, channels, and architecture for visible light communication (VLC). She is currently pursuing the Ph.D. degree with the University of M'Hamed Bougara Boumerdes. Her current

research interests include optical wireless communications, vehicular visible light communication, and energy harvesting.



**DALILA ACHELI** received the Ph.D. degree in control of systems from the University of Technology of Compiègne, France, in 1997. She is currently a Professor with the University of M'Hamed Bougara Boumerdes, Algeria. Her research interests include inverse problems, dynamic architecture, wireless networks, optical communications, evolutionary computation, and meta-heuristics.



**SELMA YAHIA** (Member, IEEE) received the B.Sc. and M.Sc. degrees in networks and telecommunications from the University of 08 Mai 1945 Guelma, Algeria, in 2017 and 2019, respectively, and the Ph.D. degree in telecommunications from the University of M'Hamed Bougara Boumerdes, Algeria, in 2023. Her research interests include optical and wireless communications, vehicular communications, visible light communication, and channel modeling.



**YASSINE MERAIHI** received the Ph.D. degree from the University of M'Hamed Bougara Boumerdes, Algeria, in 2017. He is currently an Associate Professor with the University of M'Hamed Bougara Boumerdes. His research interests include QoS for wireless networks, routing in challenged networks, including WMSNs/VANETs, and applications of meta-heuristics to optimization problems.





**AMAR RAMDANE-CHERIF** received the Ph.D. degree from Pierre and Marie Curie University, Paris, in 1998. Since 2000, he has been a Professor with the University of Versailles Saint-Quentin-en-Yvelines, France. His research interests include software architecture, dynamic architecture, architectural quality attributes, architectural styles, and design patterns.



**VAN NHAN VO** received the B.S. degree in computer science from The University of Da Nang, Da Nang, Vietnam, in 2006, the M.S. degree in computer science from Duy Tan University, Da Nang, in 2014, and the Ph.D. degree in computer science from Khon Kaen University, Thailand, in 2019. He is currently a Lecturer with Duy Tan University. His research interests include optimization, information security, physical-layer secrecy, radio frequency energy harvesting, non-orthogonal multiple access, wireless sensor networks, the Internet of Things, unmanned aerial vehicles, and the security of other advanced communication systems.



**TU DAC HO** (Senior Member, IEEE) received the M.Sc. and Ph.D. degrees in wireless communications from Waseda University, Tokyo, Japan, in 2005 and 2011, respectively. He was an Assistant Professor with Waseda University, from 2011 to 2012, a Postdoctoral Fellow with the Norwegian University of Science and Technology, from 2012 to 2014, and a Senior Researcher with SINTEF, Norway, from 2014 to 2018. He has been an Associate Professor with the Department of Electrical Engineering, Arctic University of Norway (UiT), since 2019. He joined the Department of Information Security and Communication Technology, Norwegian University of Science and Technology (NTNU), in November 2023, while he continued his position with UiT. He has participated in and led several scientific projects funded by the Norwegian Research Council and the EU Horizon, focusing on the use of ML/AI for next-generation wireless communications and networks (6G and B6G) and the applications of unmanned aerial vehicles (UAV) in those systems. He has published more than 50 international peer-reviewed publications and book chapters. His research interests include communications protocols, sustainable IoT, path planning, and optimization for radio networks with the assistance of autonomous vehicles, such as Drones/UAVs and HAPS. He has served as a committee member/reviewer for many journals of IEEE, Elsevier, Wiley, IET, IEICE, and AIAA, and flagship conferences, such as IEEE GLOBECOM, ICC, and WCNC. He is currently an Editorial Board Member of *Modern Subsea Engineering and Technology*.

...